高等学校化学学报
CHEMICAL JOURNAL OF CHINESE UNIVERSITIES
综合评述

凝聚态发光稳定有机自由基的研究进展与挑战

王圣杰, 朱子豪, 朱羽杰, 吴春晓, 阿力木·阿卜杜热合曼
(吉林大学电子科学与工程学院, 集成光电子全国重点实验室吉林大学实验区, 长春 130012)

摘要 稳定的开壳有机发光自由基由于其独特的电子结构及自旋允许的发光特性, 在光电器件、量子信息和自旋相关功能材料领域展现出重要的研究价值. 然而, 该类体系在凝聚态中普遍面临聚集诱导猝灭(ACQ)问题, 严重限制了其实际应用. 与低浓度物理掺杂等策略相比, 近年来以分子层面化学结构调控为核心的研究逐渐成为突破方向. 例如, 通过构筑自由基聚合物实现自旋中心的有效分散或借助精细分子设计调控立体位阻和分子堆积方式实现稳定高效的凝聚态发光. 本文系统总结了相关体系的光物理行为、调控机制及关键材料设计原则, 并分析了当前面临的挑战与潜在应用, 以便为发光自由基材料由基础研究迈向实际应用提供参考.

关键词 发光自由基; 凝聚态发光; 聚集诱导猝灭; 自由基聚合物; 分子结构设计
中图分类号 O631 **文献标志码** A doi: 10.7503/cjcu20250408

Advances and Challenges of Stable Organic Radicals with Luminescence in the Condensed State

WANG Shengjie, ZHU Zihao, ZHU Yujie, WU Chunxiao, ALIM Abdurahman*
(*State Key Laboratory of Integrated Optoelectronics*, *Jilin University Region*, *College of Electronic Science and Engineering*, *Jilin University*, *Changchun* 130012, *China*)

Abstract Stable organic luminescent radicals have emerged as a distinctive class of functional emitters owing to their unconventional electronic structures and spin-allowed radiative transitions, thereby enabling promising opportunities for optoelectronics, spin-related photonics, and quantum technologies. However, severe aggregation-caused quenching(ACQ) in the condensed state——driven by intensified intermolecular interactions and enhanced nonradiative deactivation——remains a major obstacle to practical implementation. Moving beyond low-loading physical doping strategies, recent advances increasingly emphasize molecular-level chemical regulation as a fundamental approach to address ACQ. Two effective directions have emerged: (i) constructing radical polymers to spatially isolate spin centers by creating protective microenvironments, and (ii) precision molecular design to tailor steric profiles and packing motifs, thereby modulating intermolecular coupling and suppressing nonradiative loss. This review summarizes the condensed-state photophysical behaviors of organic luminescent radicals, mechanistic insights into ACQ suppression and emission regulation, as well as key design principles across molecular, polymeric, and hybrid radical systems. Remaining challenges and emerging opportunities in bioimaging, optoelectronic devices, and quantum or spin-enabled applications are also discussed to facilitate the translation from fundamental studies toward practical platforms.

Keywords Luminescent radical; Condensed-state luminescence; Aggregation-caused quenching; Radical

收稿日期: 2025-12-29. 网络首发日期: 2026-02-04.
联系人简介: 阿力木·阿卜杜热合曼, 男, 博士, 教授, 主要从事有机光电功能材料与器件方面的研究. E-mail: alim@jlu.edu.cn
基金项目: 国家自然科学基金(批准号: 62422404, 52103210)和吉林省自然科学基金(批准号: 20230101363JC)资助.
Supported by the National Natural Science Foundation of China(Nos.62422404, 52103210) and the Natural Science Foundation of Jilin Province, China(No.20230101363JC).

polymer; Molecular structure design

1 Introduction

Stable organic luminescent radicals have emerged as a unique class of functional materials with distinct photophysical and spin-related characteristics[1—3]. Owing to their unconventional open-shell electronic structures and tunable spin properties, they offer opportunities for displays[4—7], sensing[8,9], and bioimaging[10—13], as well as for emerging areas in organic photonics, spintronics, and quantum information[14—21]. Recent efforts have focused on the development of efficient and stable mono- and diradical emitters, whose spin-allowed radiative transitions enable a theoretical internal quantum efficiency of up to 100%[22—30]. In particular, luminescent diradicals contain two unpaired electrons and thus exhibit a richer manifold of spin states, allowing their spin multiplicity and luminescent properties to be tuned by external stimuli such as temperature, pressure, microwave irradiation, and magnetic fields[31—35]. Despite these advantages, practical implementation is often hindered by severe aggregation-caused quenching (ACQ). Specifically, intermolecular interactions among open-shell radicals are intrinsically stronger than those in closed-shell fluorophores. As the radical concentration increases, enhanced exchange interactions between unpaired spins promote the formation of radical dimers or higher-order aggregates, which open efficient nonradiative relaxation pathways. In parallel, the delocalized electronic structures of radicals facilitate stronger π-π stacking and intermolecular charge-transfer interactions, further increasing vibrational and electronic coupling[36]. Collectively, these processes accelerate nonradiative decay, ultimately resulting in substantially reduced——or even completely quenched——emission in the condensed phase (high-concentration solutions and the solid state), severely limiting device performance[Scheme 1(A)].

To mitigate ACQ, the most widely adopted strategy to date is low-loading physical doping (typically<5%,

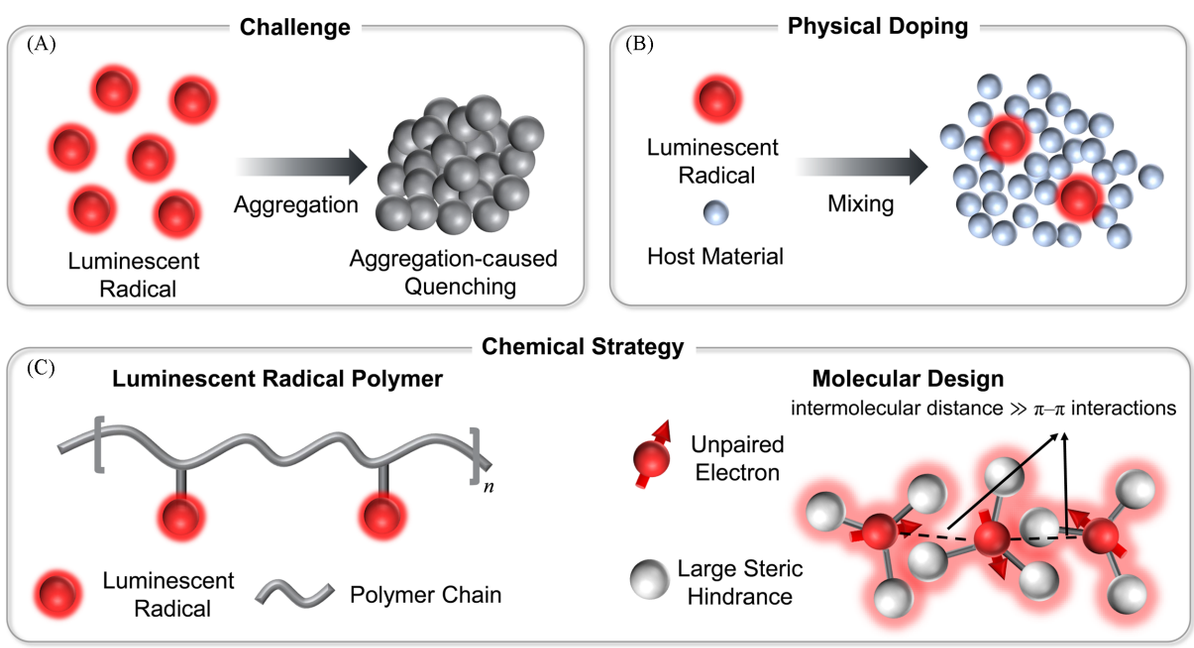

Scheme 1 Schematic of strategies for suppressing ACQ in luminescent radical systems

(A) Schematic of the ACQ phenomenon in luminescent radical systems; (B) physical doping strategy: luminescent radicals are dispersed in host materials; (C) chemical strategy; left: luminescent radical polymers(luminescent radicals are grafted onto polymer backbones); right: molecular structure design(large steric hindrance groups enhance the steric hindrance of radical centers and weaken conjugated interactions between adjacent spin centers, maintaining an intermolecular distance ≫ π-π interactions to inhibit ACQ).

mass fraction), in which luminescent radical molecules are dispersed within a host matrix. The host provides spatial separation between radical species, partially suppressing spin-spin interactions and thereby helping to retain emission in the condensed state, as shown in Scheme 1(B)[4—7,37—40]. However, this approach is intrinsically limited by issues such as inhomogeneous dispersion, phase separation, and compromised device stability. Consequently, recent efforts have increasingly shifted toward molecular-level chemical regulation aimed at suppressing aggregation at its origin, resulting in substantial progress. Among these approaches, two strategies have proven particularly effective. First, radical polymers leverage steric hindrance from polymer backbones and/or side chains to spatially isolate radical centers, enabling efficient solid-state emission[41—47]. Second, precision molecular design incorporates bulky substituents and engineers packing motifs to weaken intermolecular coupling and reduce nonradiative losses, thereby achieving robust luminescence in the condensed phase, as illustrated in Scheme 1(C)[36].

Focusing on stable organic radical systems that exhibit luminescence in the condensed state, this review summarizes their characteristic photophysical behaviors and the mechanisms governing emission regulation, with particular emphasis on material-design strategies for achieving high-performance condensed-phase luminescence. We further discuss the key scientific and technological challenges currently limiting practical implementation, and highlight emerging opportunities in bioimaging, optoelectronic devices, and quantum- or spin-enabled applications. By integrating recent advances across representative material platforms, this review aims to distill design guidelines and provide perspectives that facilitate translation from fundamental studies toward practical applications.

2 Luminescent Radical Polymers

Grafting luminescent radical units onto polymer side chains or embedding them within polymer backbones represents an effective chemical strategy to alleviate ACQ. The polymer scaffold provides steric hindrance that spatially isolates radical centers, suppressing inter-radical aggregation and associated nonradiative decay. In addition, polymeric materials offer advantages such as excellent film-forming ability, good solubility, and high chemical robustness, collectively facilitating device fabrication and practical applications. As a result, radical polymers enable a synergistic integration of radical-based luminescence with the processability and stability inherent to polymeric materials.

Most luminescent radicals discussed in this review are derived from the "star luminescent radical" tris(2,4,6-trichlorophenyl)methyl(TTM) parent scaffold, first synthesized by Armet *et al.* in 1987[48]. TTM features a central sp^2-hybridized carbon atom covalently bonded to three symmetric 2,4,6-trichlorophenyl rings; the *ortho*-chlorine steric hindrance forces the aryl rings into a propeller-like configuration. In this structure, six *ortho*-chlorine atoms form a steric shielding effect that not only protects the central reactive carbon to suppress dimerization and oxidation, endowing TTM with excellent chemical stability, but also enables unpaired electron delocalization *via* π-conjugation across the trichlorophenyl rings, further enhancing the radical's thermodynamic stability.

In 2019, Li *et al.*[42] reported the first luminescent radical polymer, PS-CzTTM[Fig. 1(A)]. Using polystyrene(PS) as the backbone, this polymer was decorated with randomly distributed luminescent radical pendants[*ca.* 5 per polymer chain; number-average molecular weight(M_n)=3.87×10^4, polydispersity index(PDI)=1.12], thereby forming a polymeric platform that integrates paramagnetism with efficient solid-state emission. The spin-coated PS-CzTTM film exhibited a pronounced emission peak at 694 nm and a photoluminescence quantum yield(PLQY) of 24.4%[Fig. 1(B)]. Meanwhile, the material showed significantly enhanced photostability with an emission intensity half-life($t_{1/2}$, s) of 1.6×10^4 s, approximately 300 times

longer than that of the monomer TTM ($t_{1/2}$=54 s) [Fig. 1 (C)]. These results underscore the effectiveness of polymer integration in enhancing the photostability of luminescent radicals. In the following year, Li *et al.*[43] fabricated a solution-processed organic light-emitting diode (OLED) using PS-CzTTM as the emissive layer, which delivered deep-red emission at 685 nm and a maximum external quantum efficiency (EQE) of 3.0% [Fig. 1 (D)]. For the PS-CzTTM film used in the device [10%—15% (mass fraction, doped in TPBi)], the PLQY was reported to be 15.4%, while that of the neat spin-coated film was 10.9%. Notably, both in the spin-coated film and in the device configuration, this system retained the characteristic doublet emission mechanism of radicals. In contrast to conventional closed-shell emitters, radicals possess a singly occupied molecular orbital (SOMO). Upon electrical excitation, electron injection into the singly unoccupied molecular orbital (SUMO) and hole injection into the highly occupied molecular orbital (HOMO) result in the formation of a doublet exciton. The spin-allowed radiative transition from SUMO to HOMO enables, in principle, a 100% internal quantum efficiency, thereby bypassing the spin-statistical limitations associated with triplet harvesting in conventional OLED emitters. These provide strong validation of the application potential of luminescent radical polymers in OLEDs.

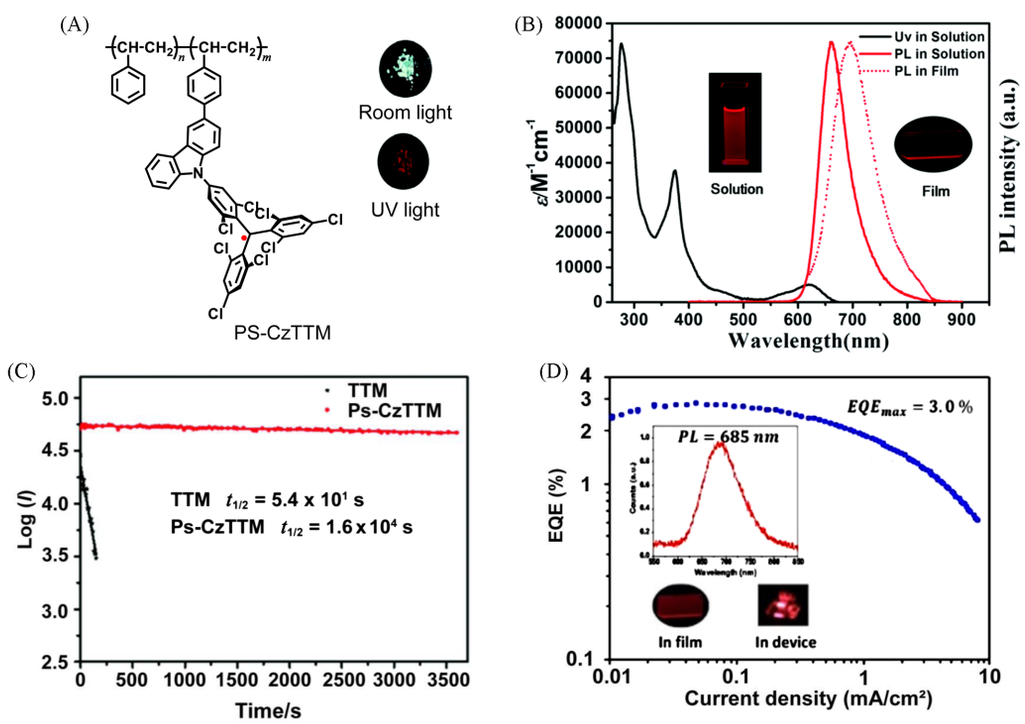

Fig. 1 Photophysical and device properties of the first luminescent radical polymer PS-CzTTM

(A) Chemical structure of PS-CzTTM and the photographs of PS-CzTTM powder under room light (up) and under UV light at 365 nm (down); (B) UV-Vis-NIR absorption spectrum (black line) and emission spectrum (red line) of PS-CzTTM in cyclohexane (1 μmol/L) and emission spectrum (red dashed line) of the PS-CzTTM in spin-coated film (100 nm, the insets); (C) comparison of the fluorescence intensity decays of TTM and PS-CzTTM in cyclohexane under irradiation with a 355 nm pulse[42]; (D) EQE of host-guest OLEDs *versus* current density[43]. Insets: (B) the photographs of PS-CzTTM in solution (left) and in the film state (right) under UV light (365 nm) at room temperature; (D) EL spectra of host-guest OLED at 12 V and the photographs of PS-CzTTM in the film state (left) and in the device (right).

(A—C) Copyright 2019, the Royal Society of Chemistry; (D) Copyright 2020, American Chemical Society.

Following the demonstration that luminescent radical polymers can effectively alleviate ACQ, research efforts have gradually shifted from merely achieving condensed-phase luminescence toward a deeper exploration of the synergistic interactions between polymer backbones and radical moieties, as well as their multifunctional application potential. In 2024, building on the previous work, Abdurahman *et al.*[44] designed

and synthesized a luminescent diradical polymer, PS-2TTM3PCz, which exhibits a markedly enhanced PLQY of 44.0% [*ca.* 1 per polymer chain; M_n=1.55×10^4, PDI=1.12] [Fig. 2(D)]. By covalently integrating a luminescent diradical monomer into the polymer main chain, the steric hindrance provided by the polymer framework not only effectively suppresses intermolecular interactions but also establishes a stable local environment for the radicals. This design enables direct investigation of the spin-state characteristics and modulation behaviors of individual diradical units.

Experimental studies revealed that the luminescence intensity of the diradical polymer PS-2TTM3PCz exhibits pronounced dependence on temperature and magnetic field [Fig. 2(E) and (F)], whereas this dependence is absent in the corresponding monoradical polymer PS-TTM3PCz [Fig. 2(A)—(C)]. However, the transient photoluminescence (PL) decay dynamics of both polymers show negligible sensitivity to temperature and magnetic field. These observations suggest that the luminescence enhancement arises from population redistribution between the ground-state singlet and triplet manifolds. Specifically, in PS-2TTM3PCz, the singlet state lies lower in energy than the triplet state and dominates at low temperatures. Increasing

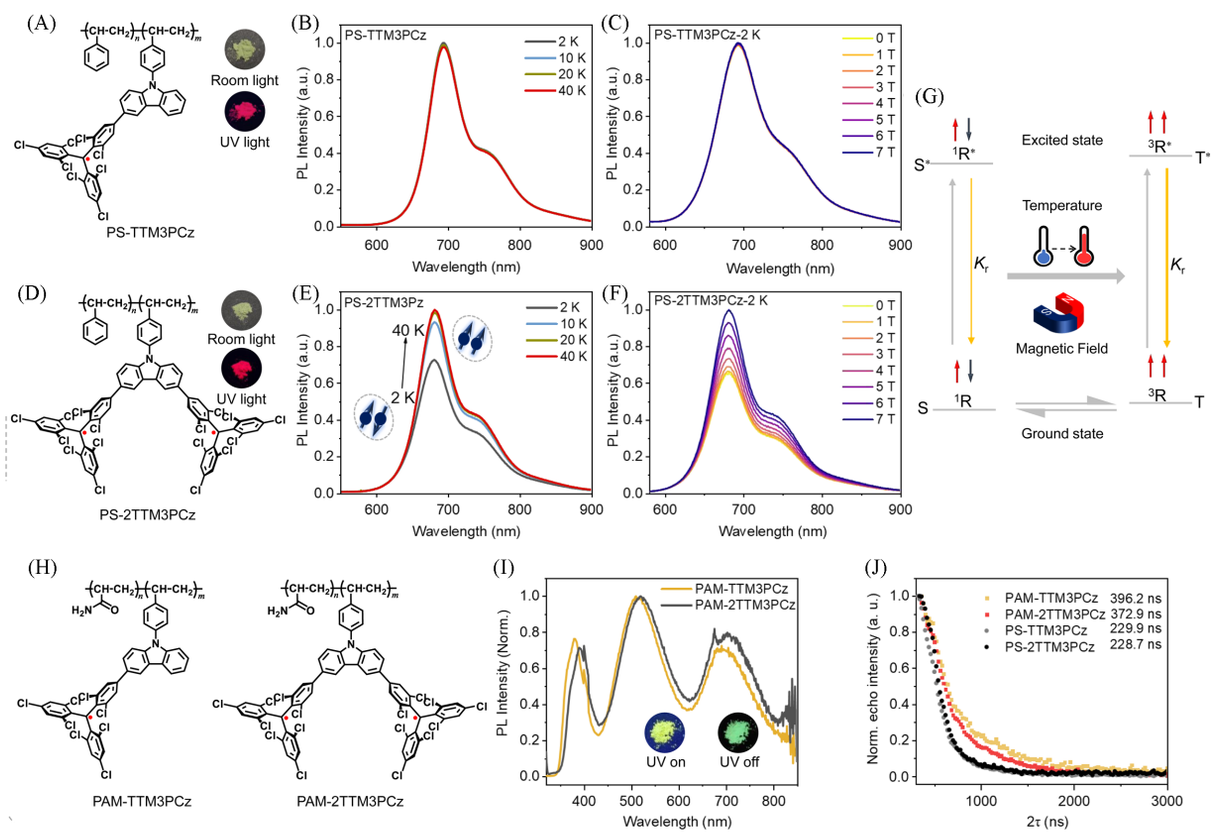

Fig. 2 Chemical structures and photophysical characterizations of luminescent radical polymer PS-TTM3PCz, PS-2TTM3PCz, PAM-TTM3PCz, and PAM-2TTM3PCz

Chemical structure and photographs of materials powder under room light (up) and under UV light at 365 nm (down) of PS-TTM3PCz (A) and PS-2TTM3PCz (D); temperature-dependent PL spectra (excitation at 375 nm) of PS-TTM3PCz (B) and PS-2TTM3PCz (E); PL spectra (excitation at 375 nm) of PS-TTM3PCz (C) and PS-2TTM3PCz (F) at different magnetic fields at 2 K; (G) temperature response and magnetic field effect luminescence mechanism of PS-2TTM3PCz[44]; (H) chemical structure of PAM-TTM3PCz and PAM-2TTM3PCz, respectively; (I) normalized steady-state PL spectra (excitation at 300 nm) of PAM-TTM3PCz and PAM-2TTM3PCz; (J) normalized Hahn-echo decay profiles of PAM-TTM3PCz, PAM-2TTM3PCz, PS-TTM3PCz and PS-2TTM3PCz at room temperature[45]. Insets of (I): photographs of PAM-TTM3PCz powder taken before (left) and after (right) switching off a 365 nm UV lamp.

(A—G) Copyright 2024, American Chemical Society; (H—J) Copyright 2024, the Authors. Published by American Chemical Society.

temperature or applying an external magnetic field promotes population of the triplet state with higher oscillator strength, leading to an overall increase in luminescence intensity[Fig.2(G)].

In 2025, Abdurahman *et al.*[45] further expanded the above-mentioned material system through a backbone engineering strategy. By selecting acrylamide (PAM), a polymer backbone favorable for room-temperature phosphorescence, and conjugating it with mono- and diradical units, they synthesized two new luminescent radical polymers, PAM-TTM3PCz and PAM-2TTM3PCz[Fig.2(H)]. Under 365 nm excitation, these materials exhibit yellow emission at room temperature, which originates from the synergistic involvement of singlet, doublet, and triplet states. After removal of the excitation source, a distinct green afterglow is observed [Fig.2(I)]. Spectral analysis indicate that radical incorporation markedly enhances triplet-state formation, providing direct experimental evidence for radical-induced excited-state intersystem crossing and its crucial role in the generation of high-spin excited states. Furthermore, pulsed electron paramagnetic resonance measurements reveal that the spin coherence time of these polymers at room temperature reaches approximately 400 ns, which is significantly superior to that of previously reported styrenyl analogs (*e. g.*, PS-TTM3PCz and PS-2TTM3PCz)[Fig.2(J)]. Collectively, these results demonstrate that the integration of multi-spin-state synergistic emission with long spin coherence times endows luminescent radical polymers with considerable potential for advanced applications, including quantum information processing and spin-photon interfaces.

With the effectiveness of luminescent radical polymers in mitigating ACQ firmly established, research efforts have increasingly focused on chemically regulating the local microenvironment and molecular structure of radicals to achieve precise control over their emission behavior. In 2022, Wang *et al.*[46] systematically investigated the role of matrix rigidity by tethering luminescent radical units onto polymer chains with varying glass transition temperatures (T_g, ℃)[Fig.3(A)]. They demonstrated that pronounced red-to-near-infrared photoluminescence in the solid state at room temperature occurs only when the T_g of the polymer matrix exceeds the ambient temperature[Figs.3(B) and (C)]. Mechanistic analyses revealed that increased matrix rigidity suppresses intramolecular vibrations and nonradiative relaxation pathways of the radicals, thereby enhancing the PLQY and lifetime (τ, ns) (the PLQY for RPE1-3 is in the range of 1.9%—2.4%, RPE4 is 10.9%, and RPE5-7 is in the range of 15.5%—16.0%). Concomitantly, the emission becomes less sensitive to temperature variations, accompanied by prolonged electron spin coherence times. In addition, the polymer matrix provides effective physical protection for the radical centers against environmental quenchers such as O_2 and H_2O, resulting in markedly improved photostability.

Beyond bulk-matrix rigidity control, microenvironment regulation can be achieved through nanoscale confinement to impart aqueous stability and bio-oriented functionality. In 2023, Kuehne *et al.*[47] introduced flexible octanoyl groups into Cz-TTM radicals and, *via* dispersion polymerization, successfully prepared monodisperse conjugated polymer nanoparticles (CPNs) that maintain stable emission in aqueous media[Fig.3(D)]. The structural and optical properties of these CPNs can be tuned by adjusting the radical monomer content and the total monomer concentration, with particle size increasing within a defined concentration range. Photophysical studies revealed that incorporation of acyl chains into the carbazole unit has little impact on the PLQY but significantly shortens the PL lifetime. For the CPNs, their PLQYs in 1-propanol range from 0.7% to 5.3% as the radical monomer ratio increases from 10% to 50% (molar fraction). Under 380 nm excitation, nanoparticles derived from oct-CzBr$_2$-TTM and dispersed in 1-propanol exhibit two distinct emission bands: intrinsic emission from the polymer backbone at approximately 450 nm and strong emission in the 655—690 nm region [Fig.3(E)]. Compared with commercially available dye-doped polystyrene particles, oct-CzBr$_2$-TTM CPNs display superior photostability and can be efficiently internalized by cells *in vitro*, demonstrating their potential as high-performance, biocompatible fluorescent imaging probes[Fig.3(F)].

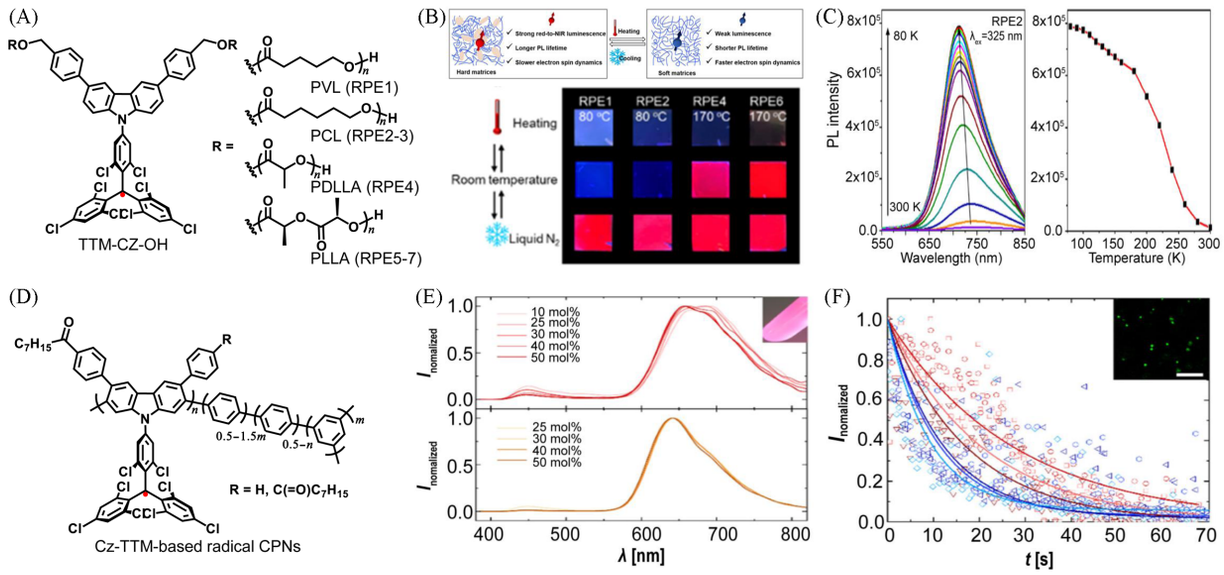

Fig. 3 Luminescence properties of diverse luminescent radical-based polymeric materials in different conditions

(A) Chemical structure of radical-centered polymers derived from TTM-CZ-OH; (B) schematic presentation to illustrate the impact of polymer rigidity on the luminescence and electron spin dynamics of the embedded radicals (up) and digital photographs of RPE1, RPE2, RPE4 and RPE6 thin films on quartz slides under UV light (365 nm, down); (C) temperature-dependent steady-state PL emission (excitation at 375 nm) spectra of the RPE2 film and the evolution of the maximal PL intensity of the RPE2 film as a function of temperature[46]; (D) chemical structure of Cz-TTM-based radical CPN; (E) PL spectra of CPN dispersions in 1-PrOH synthesized with different initial radical monomer contents of oct-$CzBr_2$-TTM and bisoct-$CzBr_2$-TTM in molar fraction; (F) PL intensity of radical CPNs made from 50% (molar fraction) oct-$CzBr_2$-TTM (red) and latex reference particles loaded with commercial red dye (blue) as a function of time. Both particle dispersions are illuminated with a 5.1 mW CW-laser at 561 nm, and three distinctive particles of both batches are recorded over time; the straight lines show an exponential fit of the data, the inset shows a confocal image of the stable aqueous dispersion of the luminescent open-shell CPNs[47]. Inset of (E): photograph of a radical CPN dispersion under UV light synthesized with the same parameters as used for the kinetic study.

(A—C) Copyright 2022, American Chemical Society; (D—F) Copyright 2023, the Authors. Published by American Chemical Society;

Importantly, polymer environments can go beyond stabilizing intrinsically emissive radicals and may even "activate" radicals that are non-emissive in their molecular form through aggregation-mediated interactions. In 2022, Tang *et al.*[49] reported that the non-emissive GTEMPO could be transformed into a red-emissive species through simple ring-opening polymerization, yielding a stable nonconjugated, nonaromatic luminescent radical polymer, PGTEMPO [Fig. 4(A)]. Unlike most luminescent radical polymers, this system exhibits typical aggregation-induced emission (AIE) behavior, in which luminescence predominantly originates from intermolecular interactions in the aggregated state rather than from isolated molecules[50—52]. Under 532 nm excitation, PGTEMPO displays a red emission band centered at 635 nm in the solid state, with PLQY of 1.3% and τ of 0.198 ns [Fig. 4(B)]. Monte Carlo simulations revealed that thermal annealing induces the formation of a continuous percolation network among TEMPO units, thereby facilitating charge transport. Consistently, Joo *et al.*[53] and Lutkenhaus *et al.*[54] reported a pronounced increase in the electrical conductivity of PGTEMPO after annealing, indicating enhanced spatial interactions within the system. This mechanism accounts for the annealing-induced enhancement of PL intensity and is further supported by the real-time red shift of the emission peak from approximately 635 to 647 nm during the annealing process [Fig. 4(C) and (D)]. Furthermore, encapsulation of PGTEMPO *via* a nanoprecipitation method enabled its application as a fluorescent

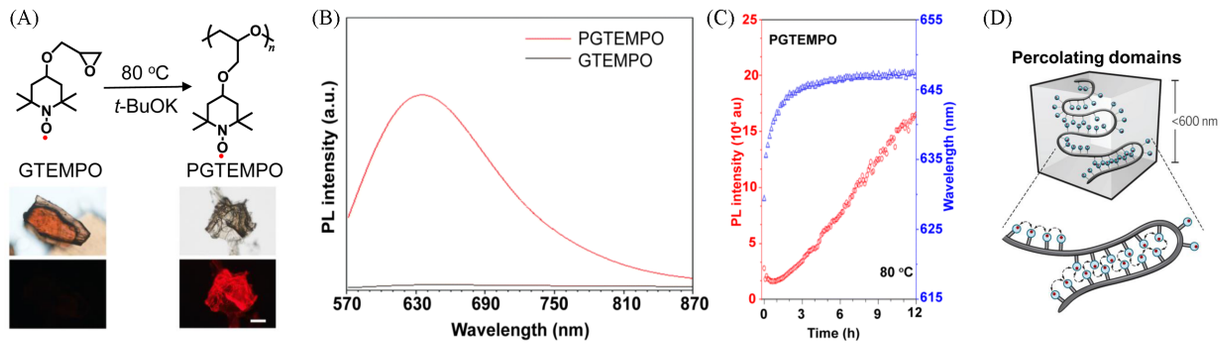

Fig. 4 Synthesis and photophysical properties of radical polymer PGTEMPO

(A) Synthetic route of the PGTEMPO radical polymer and its photos taken under ambient light (up) and 510—550 nm excitation (down); (B) PL spectra of PGTEMPO and GTEMPO in the solid state (excitation at 532 nm); (C) the real-time annealing of PGTEMPO at the temperature of 80 ℃ under nitrogen (excitation at 532 nm)[49]; (D) schematic of percolating domains after annealing[54]. (A, B, C) Copyright 2022, the Royal Society of Chemistry; (D) Copyright 2018, the Authors, some rights reserved; exclusive licensee American Association for the Advancement of Science.

sensor for antioxidant detection, demonstrating its potential for biomedical applications, including intracellular antioxidant sensing.

Extending the microenvironment-regulation concept beyond purely organic matrices, coordination systems offer an alternative platform in which organic radical ligands are assembled with paramagnetic metal ions to form coordination polymers that can also sustain radical luminescence in the aggregated state. In 2021, Kusamoto *et al.*[55] constructed and characterized a two-dimensional (2D) coordination polymer, trisZn, based on the trisPyM ligand. This material adopts a slightly distorted honeycomb structure and exhibits high structural stability. Under solid-state conditions at 79 K, trisZn displays red emission centered at 695 nm (PLQY= 3.4%), with the emission intensity gradually decreasing upon increasing temperature. Notably, trisZn also exhibits excellent photostability in the solid state. As a result, trisZn represents a class of 2D coordination polymers that integrate luminescence with unpaired electron spins, providing an ideal model system for probing the intrinsic interplay between emission behavior and magnetism.

3 Molecular Design of Solid-state Luminescent Radicals

While dispersing radical molecules in polymers can partially suppress the ACQ effect of organic luminescent radicals and enable their solid-state emission, this strategy inherently relies on diluting or confining the radicals within an inert host matrix. Achieving highly efficient solid-state emission purely from the radical material itself, without any exogenous matrix, remains a fundamental challenge and a critical step toward practical applications.

In 2018, Nishihara *et al.*[56] directly observed emission from bisPyTM crystals with an emission peak at 712 nm under 77 K, providing the first unequivocal evidence for solid-state emission from pure radical materials. Subsequently, Kusamoto and co-workers[57] reported crystal emission from the radical molecule metaPyBTM at both 77 K and room temperature. A common feature of these two early studies is that their crystal structures, through specific molecular packing, increase the distance between radical centers to approximately 0.7—0.8 nm. This effectively exceeds the typical range of π-π interactions, thereby suppressing ACQ and enabling solid-state emission *via* the formation of exciplexes. Building on this rationale, subsequent studies have further demonstrated, through more sophisticated molecular engineering, how to actively modulate the aggregate-state emission behavior of radical molecules.

In 2024, Murto *et al.*[58] systematically introduced various methylphenyl substituents into the classic

luminescent radical skeleton TTM[Fig. 5(A)], skillfully leveraging steric groups to simultaneously modulate both excited-state symmetry breaking and the degree of molecular aggregation. In the case of *ortho*-methylphenyl-substituted 2-T_3TTM, the substituent induces concerted conformational distortion in the excited state *via* steric hindrance, thereby reducing molecular symmetry and lifting the degeneracy of transition dipole moments. This results in a high PLQY of 65% at 612 nm in solution. Meanwhile, the moderate steric hindrance guides orderly molecular packing in the crystal without completely preventing aggregation, leading to a redshift of the emission spectrum to 706 nm[Fig. 5(B)]. This emission exhibits distinct exciplex characteristics, while the solid-state luminescence efficiency remains at 25%. By applying a moderate steric group strategy to achieve controlled aggregation, this work transforms typically quenching intermolecular interactions into an effective pathway for long-wavelength emission and offers new insights into the development of solid-state and near-infrared luminescence in pure radical materials.

Building on this concept, Bronstein *et al.*[59] had systematically extended and deepened this design logic, gradually evolving a general strategy of suppressing aggregation *via* spatial steric hindrance while modulating emission through conjugated aggregation. Their approach first introduces a mesityl group at the *para*-position of the TTM radical, which serves as a synthetic protecting group by occupying reactive sites, reducing side reactions during polymerization, and enabling the synthesis of polymers with high yield and well-defined structures. Simultaneously, the mesityl group provides molecular-level spatial isolation, mitigating close packing in the solid state. Donor units, such as carbazole and fluorene, are then covalently linked to construct

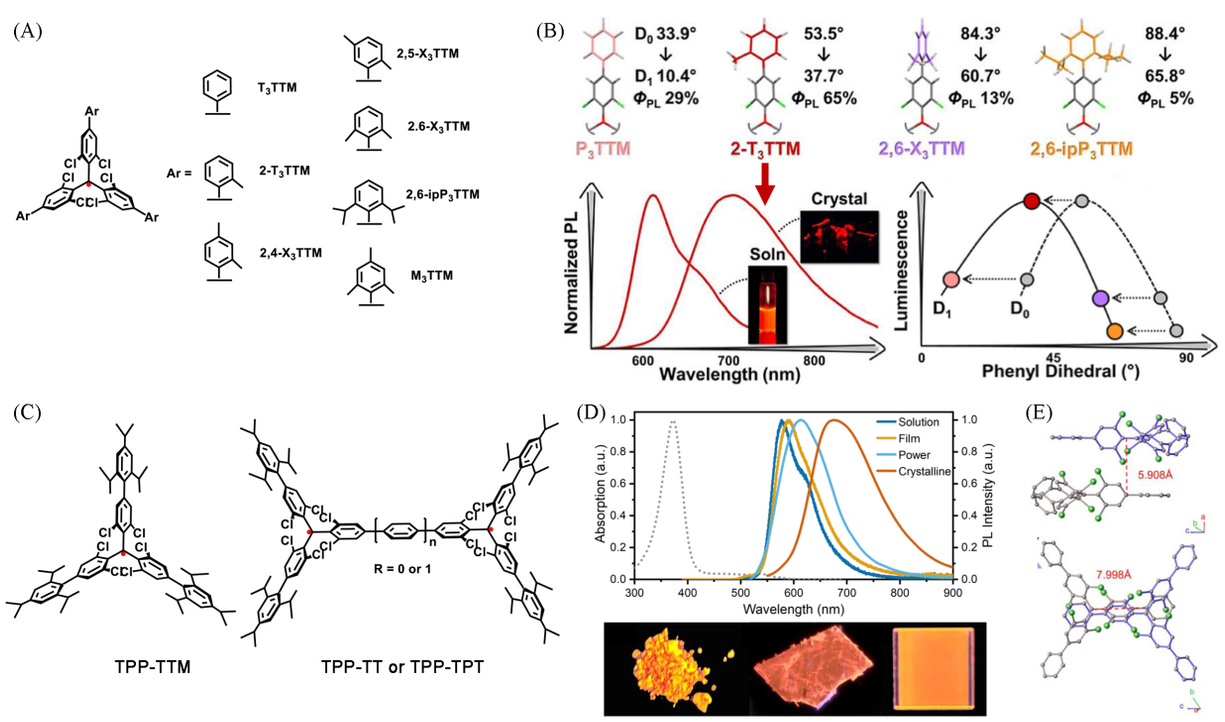

Fig. 5 Luminescence of an isolated radical molecule in the condensed state

(A) Chemical structures of TTM-based radicals; (B) molecular structures from X-ray crystal structures of the synthesized P_3TTM, 2-T_3TTM, and 2,6-X_3TTM and 2,6-ipP_3TTM radicals with average phenyl-phenyl dihedrals and emission spectrum of 2-T_3TTM in solution and in crystal[58]; (C) chemical structure of TPP-TTM, TPP-TT and TPP-TPT; (D) normalized UV-Vis absorption and PL spectra of TPP-TTM in cyclohexane solution (1×10^{-5} mol/L) and aggregated states at room temperature (up); photographs of powders, a single crystal, and a spin-coated neat film of TPP-TTM under UV light (365 nm, down); (E) front (up) and top (down) view of possible intermolecular dimer of TPP-TTM in crystals[36]. Insets of (B): the photographs of 2-T_3TTM in solution (left) and in the crystal (right).

(A, B) Copyright 2024, the Authors, published by American Chemical Society; (C—E) Copyright 2025, Wiley-VCH.

main-chain conjugated polymers. Leveraging the conformational constraints and spatial blocking effects of the polymer chains, the radical luminescent centers are effectively separated, achieving efficient luminescence in undoped pure thin films. Representative examples include the radical polymers PCzMTTM (λ_{PL}=687 nm, PLQY=10%) and PFMTTM (λ_{PL}=808 nm, PLQY=13%). Furthermore, employing rigid planar π-bridged linkers, such as 4*H*-cyclopenta[2,1-b:3,4-b′]dithiophene(CDT), to connect TTM units not only extends the emission into the second near-infrared window(1050 nm) through strong electronic delocalization, but also induces a unique luminescence mechanism[60]. The resulting highly delocalized electronic structure endows the lowest excited state with zwitterionic singlet character while imparting antiferromagnetic coupling and stable electrochromic properties. This strategy expands the material's functionality from single-component luminescence to applications in spintronics and smart displays.

In the aforementioned works, aryl electron-donating substituents such as methylphenyl and mesityl exert regulatory effects in two key aspects: in terms of steric hindrance, they impart moderate steric bulk *via* methyl substitution, affording modest spatial isolation of radical centers; in terms of electronic effects, they enhance charge transfer through π-conjugation and electron-donating inductive effects, thereby facilitating excited-state symmetry breaking. In contrast, in 2025, Abdurahman *et al.*[36] proposed a distinct design strategy: by introducing a bulky, non-conjugated 2,4,6-triisopropylphenyl(TPP) group, harmful aggregation is fundamentally suppressed sterically and electronically, thereby preserving the intrinsic luminescence of the radical in the condensed state. TPP-TTM[Fig. 5(C)], designed based on this strategy, exhibits emission spectra in various solid-state forms, such as powder and amorphous pure films, that closely resemble its solution-state spectrum[Fig. 5(D)]. This represents the first achievement of condensed-state luminescence predominantly from the monomeric state in a pure radical material. Notably, its solid-state PLQY exceeds those in solution, reaching 17.3% in powder and 18.3% in crystal, primarily due to restricted molecular motion that effectively suppresses non-radiative decay. The success of this strategy stems from the dual regulatory role of the TPP group. In contrast to the "aryl electron-donating substituents" described in prior studies, TPP exhibits notable differences in its structure-property relationships. On one hand, its substantial steric bulk forces the molecule into a propeller-like conformation with a nearly 90° twist, stabilizing the distance between molecular centers above 0.79 nm across aggregated states, well beyond the effective range of π-π stacking interactions. On the other hand, its non-conjugated isopropyl side chains significantly weaken electronic coupling between adjacent molecules. It is worth noting that a redshift of the emission peak to 675 nm is still observed in TPP-TTM crystals, likely due to the formation of head-to-tail stacked dimers in the crystal lattice, whose enhanced intermolecular charge transfer leads to exciplex formation[Fig. 5(E)]. This design strategy also demonstrates excellent generality. Extending it further to diradical systems such as TTM-TTM and TTM-PhTTM produced TPP-TT and TPP-TPT[Fig. 5(C)], which also achieve efficient and spectrally stable intrinsic luminescence in the condensed state. These results fully validate the universal value of this steric engineering for addressing ACQ in radical materials.

4 Summary and Outlook

In this minireview, we focus on the challenge of ACQ in stable organic luminescent radicals in the condensed phase, systematically summarizing recent strategies based on chemical structure modulation and highlighting two key approaches. First, the construction of radical polymers leverages steric hindrance from polymer chains to achieve effective spatial dispersion of radical spin centers. Second, precision molecular design introduces bulky substituents and tailors molecular packing modes to attenuate strong intermolecular interactions at the molecular level, thereby suppressing nonradiative decay. These efforts not only elucidate

the unique photophysical behaviors and modulation mechanisms of ACQ-suppressed radical systems but also demonstrate their potential in optoelectronic devices, bioimaging, and spin-related functional materials.

Importantly, the fundamental scientific value of stable organic luminescent radicals in the condensed phase does not lie in reproducing the performance of conventional closed-shell luminescent materials, but lies in introducing spin degrees of freedom that are inherently absent in closed-shell systems. This distinctive feature opens a new dimension for the design and regulation of photofunctional materials and enables access to spin-dependent photophysical processes beyond the intrinsic limitations of traditional systems.

Despite significant progress in suppressing ACQ and achieving efficient condensed-phase luminescence, the translation of this field from fundamental research to practical applications still faces three major challenges.

First, limited material diversity constrains mechanistic understanding. Most reported luminescent radical materials rely heavily on TTM-centered radicals, resulting in a pronounced lack of structural and compositional diversity. Additionally, research on luminescent radicals in the condensed phase is still in its infancy, with insufficient systematic screening and optimization of high-performance substituents. Expanding the material landscape through targeted molecular and materials development is therefore essential, both to elucidate fundamental regulatory mechanisms and to improve luminescence performance in the condensed phase. Specifically, in the polymer field, backbone structures are mostly confined to a few classical units, and there is an urgent need to further expand the diversity of backbone architectures. In the small-molecule realm, sterically hindered non-conjugated groups(*e. g.*, TPP) mitigate aggregation-induced emission quenching by suppressing intermolecular exchange interactions and reducing electronic orbital coupling between adjacent groups. However, systematic screening of such substituents has not yet yielded universal molecular design principles. Thus, targeted molecular and materials development based on these insights is crucial to expand the material library.

Second, the PLQY and environmental stability of luminescent radicals remain below the thresholds required for practical deployment. Further enhancement is needed to meet the stringent demands of real-world applications. For bioimaging probe applications, it is necessary to enhance the solid-state PLQY to meet the signal intensity requirements of bioimaging. For high-performance optoelectronic device applications, precise design of polymer backbones is required to balance the spatial isolation of radical emissive centers and charge transport efficiency, thereby laying the foundation for improved device performance.

Third, there is a mismatch between material development and application-driven requirements. Current research predominantly emphasizes characterization of intrinsic material properties, while exploration of application scenarios remains largely at the proof-of-concept stage. Targeted optimization toward specific requirements, such as biocompatibility for bioimaging or long spin coherence times for quantum information processing, has been limited, leaving a substantial gap between demonstrated performance and practical needs.

Looking ahead, with the continued refinement of precise molecular design and microenvironmental regulation strategies, condensed-phase luminescent radicals are expected to offer unique advantages in cutting-edge areas such as bioimaging, quantum information processing, spintronics, and spin-photon interfaces. Future research should strategically address the aforementioned core challenges and pursue three complementary directions: expanding the material landscape, optimizing key performance metrics, and advancing application-oriented studies. These efforts will facilitate the substantive translation of this field from fundamental studies to practical and scalable applications.

References

[1] Mizuno A., Matsuoka R., Mibu T., Kusamoto T., *Chem. Rev.*, **2024**, *124*(3), 1034—1121

[2] Abdurahman A., Peng Q. M., *Chin. J. Luminesc.*, **2024**, *45*(2), 211—214
[3] Straub D., Gross M., Arnold M. E., Zolg J., Kuehne A. J. C., *Beilstein J. Org. Chem.*, **2025**, *21*, 964—998
[4] Peng Q. M., Obolda A., Zhang M., Li F., *Angew. Chem. Int. Ed.*, **2015**, *54*(24), 7091—7095
[5] Ai X., Evans E. W., Dong S. Z., Gillett A. J., Guo H. Q., Chen Y. X., Hele T. J. H., Friend R. H., Li F., *Nature*, **2018**, *563*, 536—540
[6] Abdurahman A., Hele T. J. H., Gu Q. Y., Zhang J. B., Peng Q. M., Zhang M., Friend R. H., Li F., Evans E. W., *Nat. Mater.*, **2020**, *19*, 1224—1229
[7] Ai X., Chen Y., Feng Y., Li F., *Angew. Chem. Int. Ed.*, **2018**, *57*(11), 2869—2873
[8] Qu Y. Y., Li Y. C., Tan X. L., Zhai W. X., Han G. F., Hou J. L., Liu G. Q., Song Y. G., Liu Y. P., *Chem. Eur. J.*, **2019**, *25*(33), 7888—7895
[9] Zhao Y. H., Abdurahman A., Zhang Y. M., Zheng P., Zhang M., Li F., *CCS Chem.*, **2022**, *4*(2), 722—731
[10] Zhou Z. B., Yang K., He L., Wang W., Lai W. M., Yang Y. H., Dong Y. G., Xie S., Yuan L., Zeng Z. B, *J. Am. Chem. Soc.*, **2024**, *146*(10), 6763—6772
[11] Feng L., Tuo Y. Y., Wu Z. P., Zhang W. J., Li C. B., Yang B., Liu L. X., Gong J. Y., Jiang G. Y., Hu W., Tang B. Z., Wu L. M., Wang J. G., *J. Am. Chem. Soc.*, **2024**, *146*(47), 32582—32594
[12] Chen D. J., Xu Y. X., Wang Y. T., Li X., Yin D. L., Yan L. F., *ACS Appl. Mater. Interfaces*, **2024**, *16*(44), 59907—59920
[13] Liu T., Zhu Z. H., Wang S. J., Shen L., Abdurahman A., Liu X. M., Lu G. Y., *Light Sci. Appl.*, **2025**, *14*, 289
[14] Kimura S., Matsuoka R., Kimura S., Nishuhara H., Kusamoto T., *J. Am. Chem. Soc.*, **2021**, *143*(15), 5610—5615
[15] Gorgon S., Ly K., Grüne J., Drummond B. H., Myers A. W. K., Londi G., Ricci G., Valverde D., Tonnellé C., Murto P., Romanov A. S., Casanova D., Dyakonov V., Sperlich A., Belionne D., Olivier Y., Li F., Friend R. H., Evans E. W., *Nature*, **2023**, *620*, 538—544
[16] Kopp S. M., Nakamura S., Phelan B. T., Poh Y. R., Tyndall S. B., Brown P. J. J., Huang Y. H., Yuen-Zhou J., Krzyaniak M. D., Wasielewski M. R., *J. Am. Chem. Soc.*, **2024**, *146*(40), 27935—27945
[17] Poh Y. R., Morozov D., Kazmierczak N. P., Hadt R. G., Groenhof G., Yuen-Zhou J., *J. Am. Chem. Soc.*, **2024**, *146*(22), 15549—15561
[18] Kopp S. M., Nakamura S., Poh Y. R., Peinkhofer K. W. R., Phelan B. T., Zhou J. Y., Krzyaniak M. D., Wasielewski M. R., *J. Am. Chem. Soc.*, **2025**, *147*(26), 22951—22960
[19] Chowdhury R., Murto P., Panjwani N. A., Sun Y., Ghosh P., Boeije Y., Cordeiro C. D., Derkach V., Woo S., Millington O., Congrave D. G., Fu Y., Mustafa T. B. E., Monteverde A., Cerdá J., Londi G., Behrends J., Rao A., Belionne D., Chepelianskii M., Bronstein H., Friend R. H., *Nat. Chem.*, **2025**, *17*, 1410—1417
[20] Schäffer D., Wischnat J., Tesi L., de Sousa J. A., Little E., McGuire J., Mas-Torrent M., Rovira C., Veciana J., Tuna F., Chilvers N., Van Slageren J., *Adv. Mater.*, **2023**, *35*(38), 2302114
[21] Chen S. Y., Zhu Z. H., Zhou L. P., Huang H. X., Abdurahman A., Qiao X. F., Ma D. G., *J. Phys. Chem. Lett.*, **2025**, *16*(36), 9401—9407
[22] Tang B. Z., *Chem. J. Chinese Universities*, **2019**, *40*(7), 1793
[23] Li L., Prindle C. R., Shi W. Z., Buckolls C., Venkataraman L., *J. Am. Chem. Soc.*, **2023**, *145*(33), 18182—18204
[24] Hackney H. E., Ruchlin C., Stahle E., Perepichka D. F., *Angew. Chem. Int. Ed.*, **2025**, *64*(37), e202512411
[25] Li S. Z., Zhao X. L., Shi X. L., Yang H. B., *J. Am. Chem. Soc.*, **2025**, *147*(38), 34498—34507
[26] Wu C. X., Ai X., Chen Y. X., Cui Z. Y., Li F., *Chem. J. Chinese Universities*, **2020**, *41*(5), 972—980
[27] Yang Y. M., Qiu L. L., Shi X. L., *Chem. Res. Chinese Universities*, **2023**, *39*(2), 197—201
[28] Abdurahman A., Wang J. M., Zhao Y. H., Li P., Shen L., Peng Q. M., *Angew. Chem. Int. Ed.*, **2023**, *62*(15), e202300772
[29] Zhu Y. J., Zhu Z. H., Wang S. X., Peng Q. M., Abdurahman A., *Angew. Chem. Int. Ed.* , **2025**, *64*(10), e202423470
[30] Liu C. H., He Z. C., Ruchlin C., Che Y. X., Somers K., Perepichka D. F., *J. Am. Chem. Soc.*, **2023**, *145*(29), 15702—15707
[31] Matsuoka R., Kimura S., Miura T., Ikoma T., Kusamoto T., *J. Am. Chem. Soc.*, **2023**, *145*(25), 13615—13622
[32] Abdurahman A., Shen L., Wang J. M., Niu M. L, Peng Q. M., Wang J. P., Lu G. Y., *Light Sci. Appl.*, **2023**, *12*, 272
[33] Mizuno A., Matsuoka R., Kimura S., Ochiai K., Kusamoto T., *J. Am. Chem. Soc.*, **2024**, *146*(27), 18470—18483
[34] Wang X., Wang S. J., Ding Z. Z., Shen L., Zhu Z. H., Abdurahman A., Lu G. Y., Peng Q. M., *Angew. Chem. Int. Ed.*, **2025**, *64*(40), e202515393
[35] Tong Z. K., Zhang S., Niu W. W., Yu T. X., Zhang X. F., Yao P. L., Wang J. F., Han Y. B., Li G. W., Dong S. Q., *J. Am. Chem. Soc.*, **2025**, *147*(43), 39232—39246
[36] Guan J. H., Zhu Z. H., Gou Q. Q., Wang J. M., Kuang Z. Y., Zhang L. T., Zhang X. W., Ai X., Abdurahman A., Peng Q. M., *Aggregate*, **2025**, *6*(9), e70100
[37] Kimura S., Kusamoto T., Kimura S., Kato K., Teki Y., Nishihara H., *Angew. Chem. Int. Ed.*, **2018**, *57*(39), 12711—12715
[38] Liu C. H., Hamzehpoor E., Otsuka Y. S., Jadhav T., Perepichka D. F., *Angew. Chem. Int. Ed.*, **2020**, *59*(51), 23030—23034
[39] Zhu Z. H., Kuang Z. Y., Shen L., Wang S. J., Ai X., Abdurahman A., Peng Q. M., *Angew. Chem. Int. Ed.*, **2024**, *63*(42), e202410552
[40] Wang S. J., Wang X, Zhu Z. H., Shen L, Zhu Y. J., Abdurahman A., Ma H. W., Peng Q. M., Lu G. Y., *CCS Chem.*, **2025**, e202506229

[41] Zhang Z. T., Zhang J. Y., Sun J. Z., Zhang H. K., Zhang X. H., Tang B. Z., *Chem. Eur. J.*, **2025**, *31*(4), e202403493
[42] Abdurahman A., Peng Q. M., Ablikim O., Ai X., Li F., *Mater. Horiz.*, **2019**, *6*, 1265—1270
[43] Gu Q. Y., Abdurahman A., Friend R. H., Li F., *J. Phys. Chem. Lett.*, **2020**, *11*(14), 5638—5642
[44] Wang S. J., Wang X., Ding J. S., Zhu Z. H., Wang J. M., Shen L., Abdurahman A., Lu G. Y., Wang J. P., Peng Q. M., *Macromolecules*, **2024**, *57*(13), 6133—6139
[45] Wang S. J., Zhu Z. H., Abdurahman A., Peng Q. M., *Macromolecules*, **2025**, *58*(1), 372—378
[46] Hou L. M., Xu H. X., Zhang X. Y., Zhang Y. P., Chen R., Zhang Z. Y., Wang M. F., *Macromolecules*, **2022**, *55*(19), 8619—8628
[47] Chen L., Rudolf T., Blinder R., Suryadevara N., Dalmeida A., Welscher P. J., Lamla M., Arnold M., Herr U., Jelezko F., Ruben M., Kuehne A. J. C., *Macromolecules*, **2023**, *56*(5), 2104—2112
[48] Armet O., Veciana J., Rovira C., Riera J., Castaner J., Molins E., Rius J., Miravitlles C., Brichfeus S., *J. Phys. Chem.*, **1987**, *91*(22), 5608—5616
[49] Wang Z. Y., Zou X. H., Xie Y., Zhang H. K., Hu L. R., Chan C. C. S., Zhang R. Y., Guo J., Kwok R. T. K., Lam J. W. Y., Williams I. D., Zeng Z. B., Wong K. S., Sherrill C. D., Ye R. Q., Tang B. Z., *Mater. Horiz.*, **2022**, *9*, 2564—2571
[50] Chen P. Y., Zhang G. Y., Li J. G., Ma L. J., Zhou J. Y., Zhu M. G., Li S., Wang Z., *Chem. Res. Chinese Universities*, **2024**, *40*(2), 293—304
[51] Xiong J. Y., Wu M. J., Yao L. Y., *Chem. Res. Chinese Universities*, **2024**, *40*(5), 887—893
[52] Sun Z. H., Yin P. P., He S. Y., Zhang K. G., Pan X. R., Wang J. Y., Hao P. N., Zhou Z., Yang X. G., Ma L. F., Tan C. L., *Chem. Res. Chinese Universities*, **2025**, *41*(3), 519—524
[53] Joo Y., Agarkar V., Sung S. H., Savoie B. M., Boudouris B. W., *Science*, **2018**, *359*(6382), 1391—1395
[54] Lutkenhaus J., *Science*, **2018**, *359*(6382), 1334—1335
[55] Kimura S., Uejima M., Ota W., Sato T., Kusaka S., Matsuda R., Nishihara H., Kusamoto T., *J. Am. Chem. Soc.*, **2021**, *143*(11), 4329—4338
[56] Kimura S., Tanushi A., Kusamoto T., Kochi S., Sato T., Nishihara H., *Chem. Sci.*, **2018**, *9*, 1996—2007
[57] Matsuoka R., Kimura S., Kusamoto T., *ChemPhotoChem*, **2021**, *5*(7), 669—673
[58] Murto P., Li B., Fu Y., Walker L. E., Brown L., Bond A. D., Zeng W., Chowdhury R., Cho H. H., Yu C. P., Grey C. P., Friend R. H., Bronstein H., *J. Am. Chem. Soc.*, **2024**, *146*(19) 13133—13141
[59] Murto P., Chowdhury R., Gorgon S., Guo E., Zeng W. X., Li B. W., Sun Y. Q., Francis H., Friend R. H., Bronstein H., *Nat. Commun.*, **2023**, *14*, 4147
[60] Yu C. P., Chowdhury R., Fu Y., Ghosh P., Zeng W. X., Mustafa T. B. E., Grüne J., Walker L. E., Congrave D. G., Chua X. W., Murto P., Rao A., Sirringhaus H., Plasser F., Grey C. P., Friend R. H., Bronstein H., *Sci. Adv.*, **2024**, *10*(30), eado3476

(Ed.: W, K, M)